Continuous 3-D preSDM velocity analysis

Ian F. Jones, Huibert Baud, and Keith Ibbotson, CGG, Feltham, England
François Audebert, CGG, Massy, France

Over the past few years, many techniques have been presented for updating the velocity depth model required for full-volume 3-D prestack depth migration (preSDM).

These techniques (many of which are listed in "Suggestions for further reading") have specific theoretical or practical limitations. Furthermore, a universal limitation to date is the spatial sampling of the information used to perform the velocity estimation. Prestack-migrated velocity information (usually in the form of CRP gathers) is typically output on a coarse grid, often 500 × 500 m.

This article presents a technique for increasing the statistical reliability of the velocity information to be input to the chosen velocity update scheme. The automated nature of this technique greatly reduces the unreasonably high number of man-hours needed to manually pick very dense velocity grids—the factor that has really limited us in the past in obtaining dense velocity grids.

Thus, this paper does not present a new method for obtaining velocity information for preSDM model updating; it demonstrates a technique for analyzing information produced continuously. We do not in any way improve on the limitations of the underlying technique; we merely make the best possible use of the information already available by looking at a very dense sampling of information.

In other words, when we estimate the velocity with many values, we only improve the precision of that estimate—not the accuracy. Thus, if the values coming from our velocity estimator were all erroneous, but consistently erroneous, then we would simply have a very precise estimate of that inaccurate result.

The method. The basis of the new technique is derived from that described by Doicin et al. (1995). In this technique, a CMP gather is NMO-corrected and a scan of perturbed residual NMO gathers is created from it. This ensemble of moveout-corrected gathers is then input to a coherency analysis routine to determine the "best" moveout velocity on the basis of, say, stack power. This approach results in an estimate of stacking velocity at each CMP location and each time sample. In this regard, their approach was not new (see, for example, de Bazelaire, 1988). However, the important innovation by Doicin et al. was related to the statistical analysis of the infor-

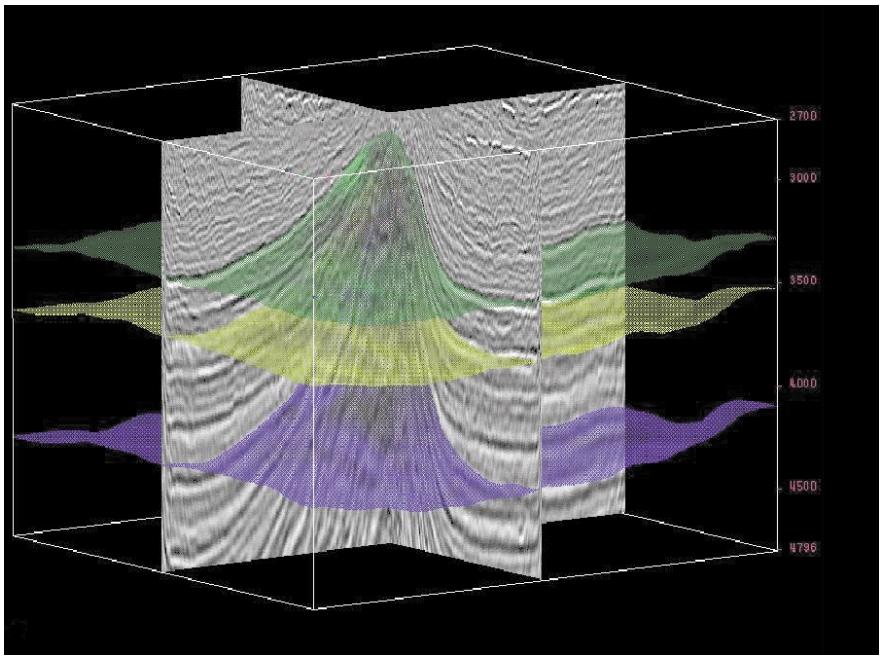

Figure 1. 3-D PetroCaem image of salt dome.

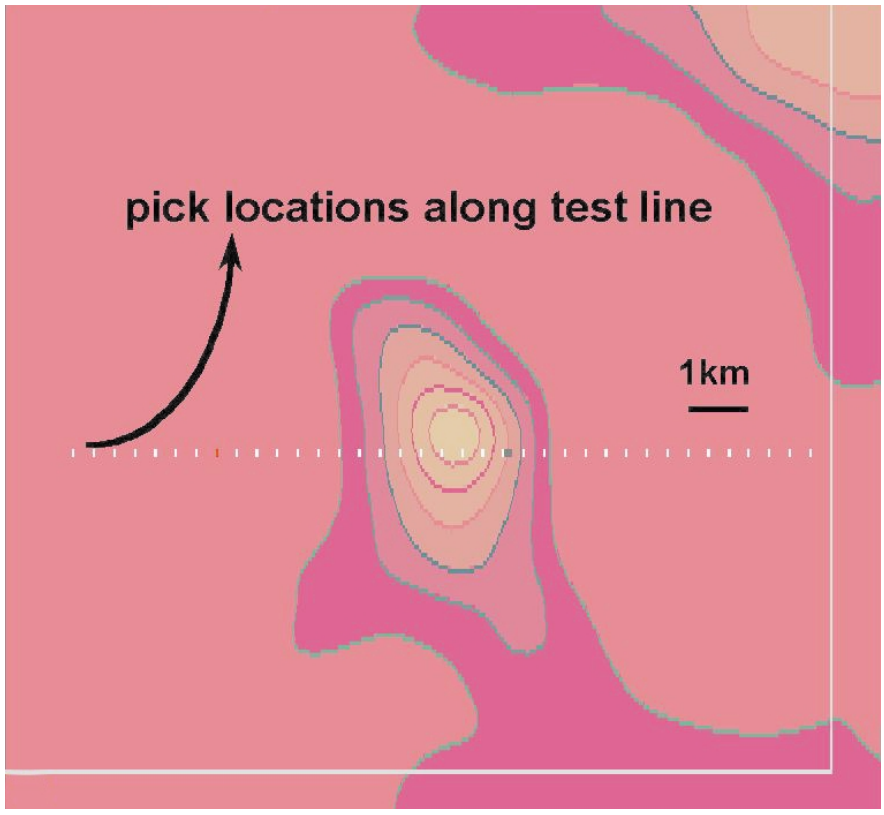

Figure 2. Depth map of BCU event.

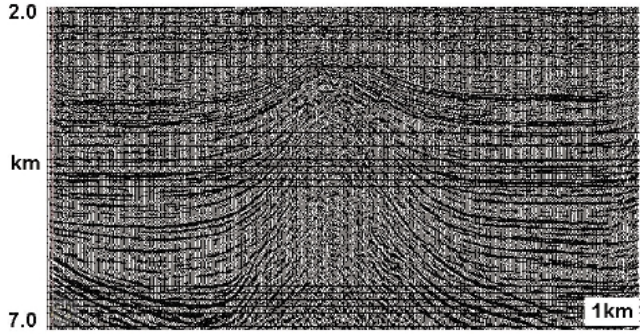

Figure 3. 3-D preSDM image resulting from final TomCad model.

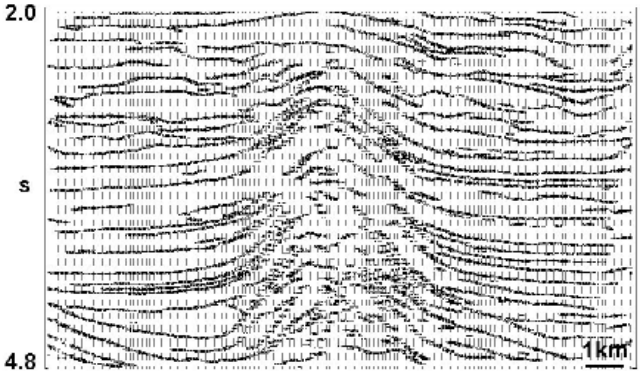

Figure 4. Autotracked event skeleton from CRP data output every 25 m (19-point operator).

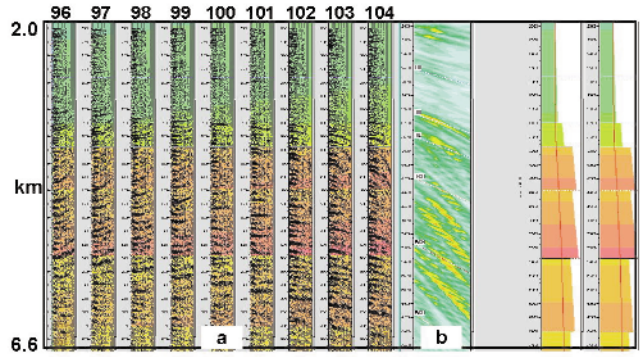

Figure 5. 3-D preSDM CRP scan and spectrum.

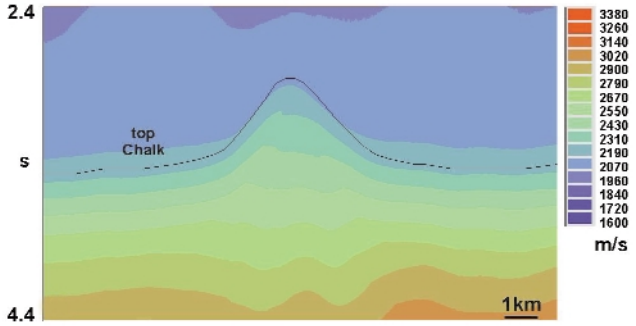

Figure 6. RMS velocity of preSDM model. 3-D tomographic inversion on 200-m grid.

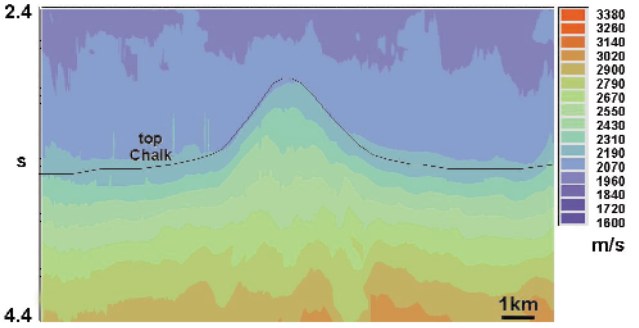

Figure 7. RMS velocity of CRP scan data. Automated output every 25 m (19-point operator).

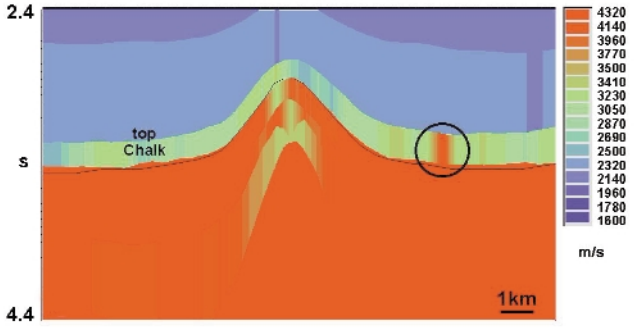

Figure 8. Interval velocity from CRP scan data. Manual picking in iso-x utility on 500 m grid.

mation produced so as to eliminate picks of peg-leg multiples and to eliminate velocity information which showed little or no spatial (geologic) coherence.

Here we describe a variant of the technique, adapted to the depth domain, that is based on the CRP-scanning technique of Audebert and Diet (1996). We do not simply introduce residual moveout into a single migrated CRP gather but compute a suite of CRP gathers at each CMP position; each gather in this "scan" results from a unique 3-D preSDM performed with a perturbed rendition of the velocity depth model. These scans are then input to a modified version of Doicin's algorithm. Again, we do not diminish the theoretical limitations of the velocity estimation scheme, but we certainly increase the reliability of the velocity information obtained.

One feature of the Doicin technique is the suppression of velocities corresponding to peg-leg multiples. When the velocity table is being computed for a given CMP (with a numerical value of velocity for each time sample), each value is assessed to see if it could correspond to a peg-leg multiple velocity. This is achieved by comparing the current velocity value with that which exists τ ms before it (where τ is the time period associated with water-bottom peg-leg multiples). If the current velocity corresponds to a peg-leg multiple of a previous velocity, then its value is deleted and replaced with the velocity corresponding to the next "most energetic" stack for this time.

After the peg-leg multiple velocities have been removed, a search is conducted to see if the same numerical value of velocity persists on adjacent CMPs (within some dip range and velocity bounds). The length of the spatial coherence gate is a parameter of the process. Values that do not display spatial coherence are deleted. The result is the "velocity skeleton" which resembles an autotracked horizon representation of the seismic section for this velocity line. We see horizons (or horizon segments) wherever we have spatially continuous velocity boundaries in the data.

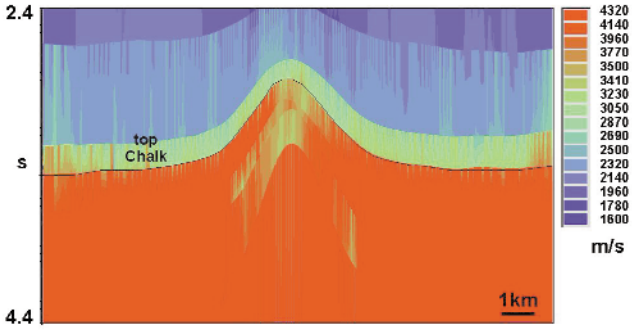

Figure 9. Interval velocity of CRP scan data. Automated output tracking horizons every 25 m (19-point operator).

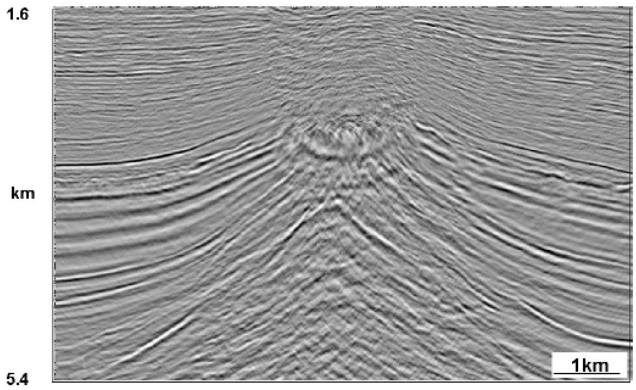

Figure 10. 3-D preSDM image from final preSDM model.

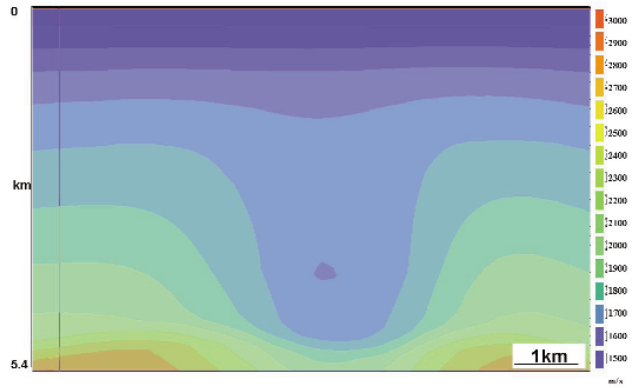

Figure 11. RMS velocity of final model.

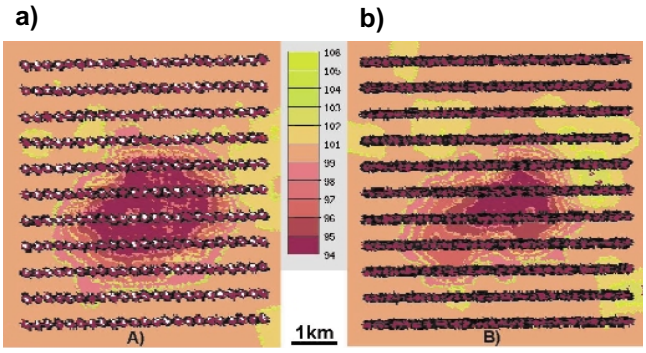

Figure 12. Perturbation picks from CRP-scan data. (a) manual picks on a 250 × 600 m grid and (b) automatic picks on a 25 × 600 m grid.

Example 1. The geologic problem involves improved imaging of salt-flank sediments. These data (courtesy of Elf Norge) were initially part of a postSDM project, where the velocity model was built via iterative 3-D tomographic inversion (TomCad) in conjunction with layer-stripping postSDM (Lanfranchi et al., 1996). Figure 1 shows a PetroCaem 3-D perspective view of the data with model horizons superimposed. These results were the starting point to investigate improvements gained by preSDM and application of the continuous preSDM velocity analysis scheme.

A single line was chosen to demonstrate the details of the continuous velocity analysis process. Figure 2 shows a depth map of the base Cretaceous unconformity (BCU) from the TomCad model and the location of the velocity line. The locations along the line are those points used for manual picking of CRP-scan gathers, every 500 m, as part of the preSDM update.

Figure 3 shows the 3-D preSDM image for this line. Figure 4 shows the velocity skeleton of these salt dome data. Each "point" in the skeleton corresponds to a location that displays lateral coherence in the velocity field. In this example, the length of the lateral coherency window was 19 CMPs. Hence, if we were to see an isolated value of velocity in this skeleton, it would tell us that there were only 19 consecutive CMPs that had approximately this velocity in the vicinity of this point. (By "vicinity," we mean within the search window on the segment being tracked.)

CGG's usual approach to updating this model would be to use CRP-scanning. Figure 5 is a scan of nine CRP gathers (corresponding to 96-104% perturbations of the current velocity model, in increments of 1%). Manual picking would be performed either on the gathers (Figure 5a) or from the spectrum (Figure 5b), typically on a grid of 500 × 500 m.

For the new technique, these scans would be produced continuously (e.g., every 25 m) along the velocity lines (spaced, for example, every 250 m), and then input to the new process for investigation for maximum "stack" power (for a given depth in the current model) and spatial coherence.

Figure 6 shows the RMS velocity corresponding to the original model derived from tomographic inversion, and Figure 7 shows the RMS velocity corresponding to the automated procedure using a 19-CMP coherence operator. An interpretation of the top-chalk event is superimposed to give geologic reference. Note that, at this stage, no model has been input to the process. The procedure is entirely automatic. It is only when we invert to interval velocities that a model is used.

Figure 8 shows the interval velocity derived from the RMS values from manual picking of CRP-scan data, with picks made every 500 m. Figure 9 shows the results from automatic picking. Here we have used simple vertical Dix inversion to convert the RMS to interval velocity using the horizons from the existing model.

Toward the center right of the horizon above the chalk is an anomalously high velocity in the layer (circled in Figure 8). This is not in keeping with the surrounding velocity field; it would appear as a bullseye in the velocity map and would probably be edited out. Thus we would have a hole in the velocity field and an associated reduction in reliability.

The automated procedure did not retain this anomalous value. The

value probably arises from small-scale faulting in this horizon, so the CRP gather at this point had the fault-plane energy dominating the velocity pick. If we compare the percentage difference between manual picking and automatic picking, we see that differences of >10% are common.

Perhaps the most important difference between the two approaches is that manual picking will take 2-3 weeks per iteration of the whole 3-D preSDM study, but the automatic approach will take about 90 s of CPU time per line. Naturally, we have more CPU overhead in computing the continuous CRP scans, but this is more than offset by the saving in man-hours. Following the picking phase of this iteration (either manual or automatic), we move to editing/smoothing/QC of the velocity field, model update, and next iteration.

We consider this reduction in man-hours to be the main benefit of this technique. As a result, the effort normally put into routine picking can now be directed into QC or other ways to speed up the project. We envisage using this technique throughout each iteration in the model-building process.

Example 2. The second example of the continuous velocity analysis technique is taken from a gas-cloud problem associated with another North Sea salt structure (courtesy of Kerr-McGee UK). Figure 10 is a preSDM seismic section from this 3-D survey. Figure 11 is a vertical RMS velocity profile from the manually picked CRP-scan model building.

Figure 12a shows the results from manual picking of model perturbations from the CRP scans for a key horizon (showing analysis locations every 250 m along velocity lines spaced every 600 m). Figure 12b shows the corresponding automated picking results (with picks every 25 m along the velocity lines).

Figures 13a and 13b show the respective interval-velocity maps after tomographic update of these velocity perturbation results and application of a low-pass spatial filter. Figure 14 shows the percentage difference between the grids. The automated velocity field has a smaller central low velocity zone (associated with the gas cloud). In other words, the automated picking was able to track meaningful values of velocity a bit further into the gas anomaly.

Another way to assess the model,

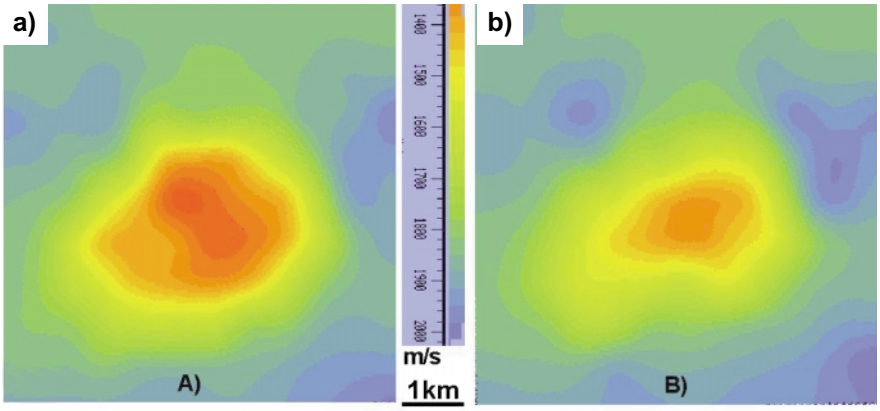

Figure 13. Raw interval velocity from tomographic update of CRP scan data. (a) Manual picking on 250 × 600 m grid and (b) automatic picking on 25 × 600 m grid.

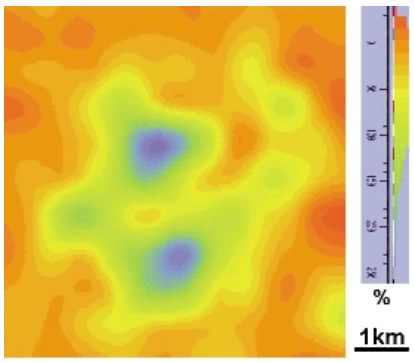

Figure 14. Percentage difference in interval velocity between manual and automated picking.

this time via the image quality, is to output the preSDM images associated with each element of the CRP scan. Given that the continuous velocity analysis technique relies on having a model perturbation scan at each CMP along the velocity line, it is helpful to output the "stacked" preSDM images associated with each element of the scan. These preSDM image scans are especially useful for complex regions or deeper parts of the data. Figure 15 shows preSDM images associated with 94%, 100%, and 106% (only end members of the scan are shown). It is clear that the fault segmentation on the base-Cretaceous event, below the gas cloud, is properly imaged in the 100% image.

An alternative approach to the automated update procedure is to pick a horizon in one of the percentage-scan images and propagate these picks to the other percentage-scan images. We can then select the maximum amplitude at each CDP location and extract the percentage velocity perturbation associated with

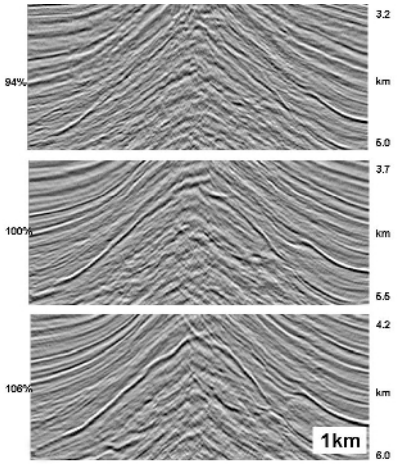

Figure 15. 3-D preSDM images from a scan of perturbed models.

this maximum in perturbed image amplitude.

Conclusions. The first part of this paper presented a new technique for continuously analyzing 3-D preSDM velocities. Although we assert that the theoretical benefit is that of improved reliability of the velocity estimates, the most practical benefit is the possibility to speed up the model-building process for those data that lend themselves to the technique. Data heavily contaminated with multiples will probably be unsuited for such automated techniques.

In addition, stacking the elements within the CRP-scan to provide a suite of 3-D preSDM-migrated images (one for each model perturbation) permits geologic insight in the QC of results, especially when there is a multiple problem and in deeper parts of the image when the CRP gathers do not contain enough velocity discrimination to permit meaningful update.

It is our contention that such techniques as this will be routinely used on all CRP gathers in preSDM surveys once machines become sufficiently cost-effective to permit whole volume velocity update instead of the present coarse velocity grid. An intermediate solution would be to apply such techniques to thin corridors of CRP data computed only in the vicinity of the model horizons (e.g., Wyatt et al., 1992).

Suggestions for further reading. "CRP-scans: 3-D preSDM migration velocity analysis via zero-offset tomographic inversion" by Audebert et al. (Proceedings of the 1997 spring symposium of the Tulsa Geophysical Society, SEG). "CRP-scans from 3-D prestack depth migration—a new tool for velocity model building" by Audebert et al. (1996 EAGE Annual Meeting). "A strategic approach to 3-D prestack depth migration" by Diet et al. (SEG 1994 *Expanded Abstracts*). "Normal moveout revisited: inhomogeneous media and curved interfaces" by de Bazelaire (GEOPHYSICS, 1988). "Common-offset migrations and velocity analysis" by Deregowski (*First Break*, 1990). "Machine guided velocity interpretation" by Doicin et al. (1995 EAGE Annual Meeting). "3-D prestack depth migration and velocity model building" by Jones et al. (*TLE*, 1998). "Enhancements to 3-D preSDM salt-flank imaging" by Jones et al. (*Journal of Seismic Exploration*, 1998). "Continuous 3-D preSDM velocity analysis" by Jones et al. (1997 EAGE Annual Meeting). "A new technique for 3-D preSDM model building: a North Sea case study" by Jones et al. (1996 EAGE Annual Meeting). "3-D velocity model building via iterative one-pass depth migration" by Jones (SEG 1993 Annual Meeting). "Model building using 3-D tomographic inversion of multiarrivals—a North Sea case study" by Lanfranchi et al. (1996 EAGE Annual Meeting). "The use of 3-D prestack depth imaging to estimate layer velocities and reflector positions" by Reshef (1994 EAEG/SEG Summer Workshop). "Ergonomics in 3-D depth migration" by Wyatt et al. (1992 SEG *Expanded Abstracts*). E

Acknowledgments: The authors thank Elf Norge and Kerr-McGee for permission to use their data. Thanks also to Bill Henry and Andy Strachan of the CGG London imaging group for their assistance.

Corresponding author: ifjones@cgg.com